DRAFT VERSION JUNE 13, 2006
Preprint typeset using LaTeX style emulateapj v. 11/26/04

METHODS OF MASKING NON-ICL LIGHT IN VIRGO IMAGES

STEVEN

Subject headings: masking

1. INTRODUCTION

Images taken around the Virgo cluster will not only contain light from the Intracluster Light but also from foreground stars (in our own galaxy) and background galaxies. As we are measuring quantities of light in the images, it is important to know which areas of the image should be included and which should be ignored in our examination. We have developed a process of masking which does a satisfactory job of eliminating the non-ICL light in the images. This process combines three separate masks: a "by hand" mask of bright stars and diffraction spikes, an automated SExtractor mask, and a surface brightness cutoff mask.

The images used for this masking are small portions of our large mosaic image as selected in the Planetary Nebulae studies of the Virgo Cluster by Feldmeier et al. (2003) and Aguerri et al. (2005). These fields are shown overlaid on our full image in Figure 1.

2. "BY HAND" MASKING

Quite noticeable around the bottom in Figure 1 are halos and spikes around the bright stars. As these would distort our measurements of light, they are masked manually as needed. Circles are placed around the bright stars to eliminate the halos around (caused by the reflection from the inside of the Schmitt Corrector). Small boxes are used to eliminate the diffraction spikes when they extended significantly beyond the halo mask. The masks are shown as dark outlines in Figure 2.

3. SEXTRACTOR MASKING

The procedure with SExtractor follows closely the method used in Feldmeier et al. (2002). As there is an amount of noise on the data, we would like to determine a cutoff magnitude that splits our data between magnitudes where the noise dominates and magnitudes where the true signal dominates. This is accomplished by using the symmetry of noise and the asymmetry of the signal in our data. However, the first step is to subtract out the large galaxies and broad, diffuse light as much as possible since we are primarily concerned here with masking out stars and small (distant) galaxies.

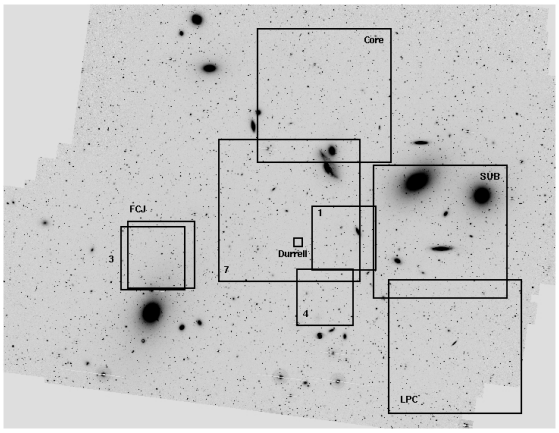

FIG. 1.— Regions selected for masking and study.

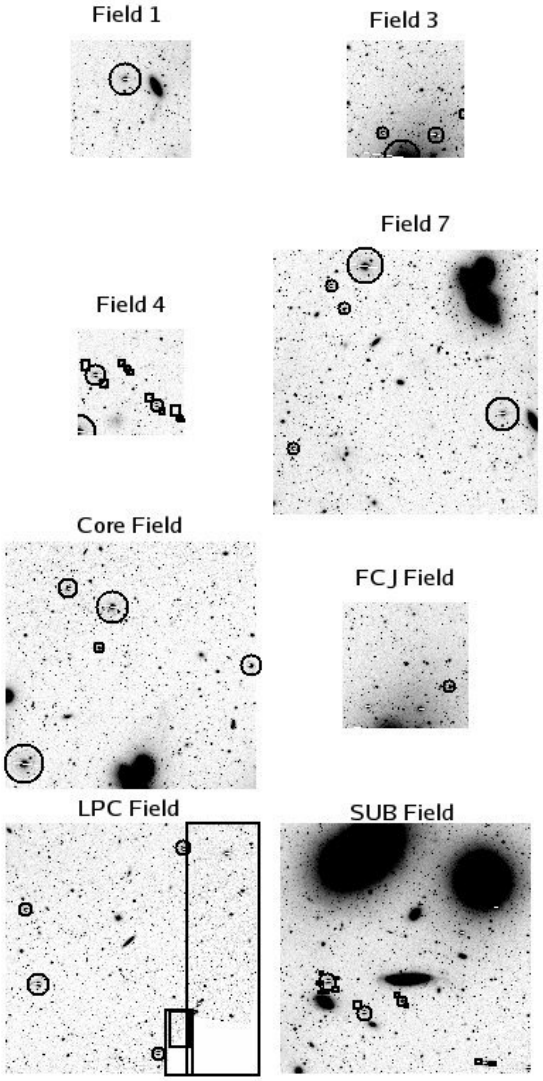

FIG. 2.— Outlines of hand-masked regions in the eight selected fields

To accomplish this, we smooth the images with IRAF's RMEDIAN ring median smoothing using an inner radius of 5 pixels and an outer radius of 9 pixels. This smoothed image was subtracted from the original image to eliminate most of the large galaxies. Figure 3 shows the Core field before and after the smoothed subtraction has been applied.

We begin the real masking procedure by running the SExtrator object detection program on each field with fairly harsh

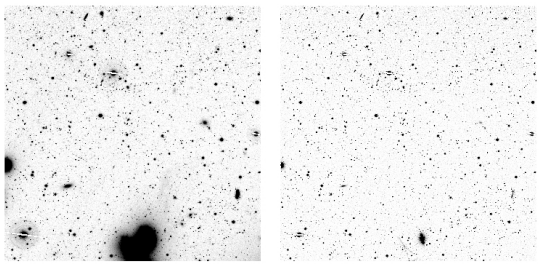

FIG. 3.— Core Field before (left) and after (right) ring-median smooth subtraction was performed

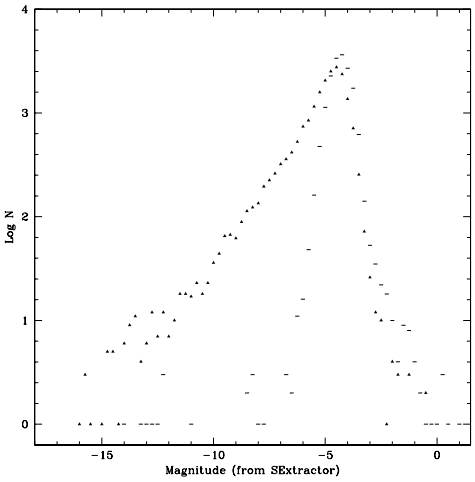

FIG. 4.— Histogram of distribution of objects detected in real and inverse images of Core field. Solid triangles represent objects detected in the original image, dashes are the objects detected in the inverse image.

running parameters - a threshold of detection at 0.6 σ above sky and a minimum detection radius of 3 pixels. We also set the deblending threshold to 32 which means objects that are close together will be considered as separate objects and not blended together. Objects that are detected at this point are caused both by signal and noise. Next the same parameters are used to detect objects on the inverse of the image. Now, however, all of the objects detected are from noise. The objects detected in both methods are collected in magnitude bins $\frac{1}{4}$ a magnitude wide. For example, the binned values for the Core field and its inverse are plotted on the same axes in Figure 4.

In this histogram, the negative noise spike and real object distributions have their peaks at similiar magnitudes and with similar Number of objects. With the relationship between these two histograms, an estimate of the data's validity is generated at a given magnitude. This is the next step - we divide the inverse histogram by the real histogram and obtain a curve that relates the combined signal and noise level to the noise level alone. Figure 5 shows this curve with our third-order polynomial best fit to it. Objects with magnitudes brighter than the scale of this plot are considered to be good objects, objects fainter than this plot are taken as noise, and not real

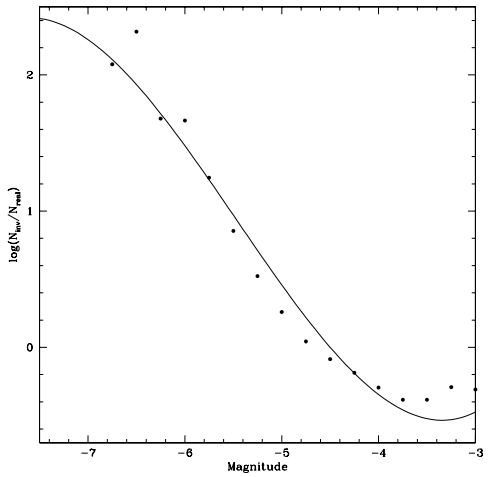

FIG. 5.— Quotient of inverse histogram and real histogram between certain limits. This curve fit indicates the likelihood that an object of a given magnitude is real or is from the noise.

objects. To determine the validity of objects that fall between these boundaries, a simple Monte Carlo technique is used. After normalising the function between these limits, it is used as a probability function that an object with a certain magnitude is real. By generating random numbers, we determine which objects should be kept and which should be ignored. After this Monte Carlo "good object" selection is completed, a mask is made that includes all of the objects identified as real - the SExtractor object mask.

4. SURFACE BRIGHTNESS MASKING

The final component of the overall mask is a cutoff in surface brightness. With a simple implementation of the IRAF tool imexprression, all pixels with surface brightnesses brighter than μ_V= 25 mag/arcsec^{2}are masked out. While many of these pixels had already been detected and masked with the SExtractor mask or were in the hand masks, this mask eliminates new pixels mostly around the bright galaxy centers which were not masked by the SExtractor mask as it is performed on the smooth subtracted image without galaxies in it. The final result for the Core field is shown in Figure 6.

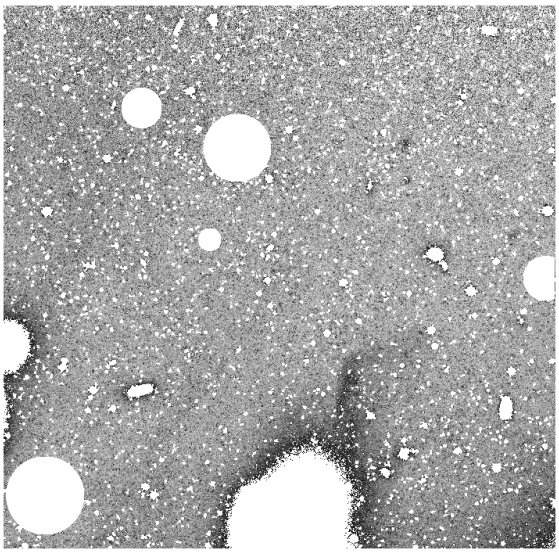

FIG. 6.— Final total mask for Core field from hand mask, SExtractor mask, and surface brightness threshold mask. Blank white areas are masked regions.